Research Article

Orhan Canbolat*, Fatih Canbolat, Mehmet Ali Ergün, Selin Yiğit and Gülendam Bozdayı

Investigation of the effect of low-power, low-frequency ultrasound application on SARS-COV-2

https://doi.org/10.1515/tjb-2023-0204
Received September 5, 2023; accepted January 2, 2024;
published online May 28, 2024

Abstract

Objectives: Numerous studies have been conducted on the prevention, diagnosis, and treatment of the SARS-CoV-2 pandemic, which remains a global health concern. Low-frequency and low-dose ultrasound can help eradicate the virus from the air and the environment. Our research aims to determine how altering ultrasonic waves frequencies and low power affects the virulence and replication rate of a virus.

Methods: The virus was identified using atomic force microscopy before the initiation of laboratory tests. The experimental environment was exposed to 8 W of ultrasound at frequencies of 40 KHz, 25, 50, and 110 MHz. The cycle threshold (Ct) of the samples before and after ultrasonography was evaluated using real-time PCR (RT-PCR). Before and during ultrasonography, the VERO E6 Cell line was employed to determine whether the virus was still alive.

Results: Following the RT-PCR results, the application of 40 KHz ultrasonic waves frequency enhanced the Ct values of the virus while concurrently inhibiting its growth rate in the cell culture.

Conclusions: Our findings suggest that employing ultrasound to eliminate SARS-CoV-2 and possibly other closed and single-stranded RNA viruses from the environment is feasible.

Keywords: SARS-cov-2; ultrasound; real-time PCR; atomic force microscopy; cell culture

Introduction

The pandemic, also known as Severe Acute Respiratory Syndrome Coronavirus-2 (SARS-CoV-2; COVID-19 illness), has caused and continues to create significant economic, social, and psychological difficulties, particularly in the realm of worldwide public health. The condition may first present as a cold, but it can progress to other organ failure and death if left untreated. After being recovered from clinical specimens, viruses' genomes were sequenced rapidly [1, 2]. To begin, SARS CoV-2 is a large, enveloped, positive-stranded RNA virus. Genomes of these organisms generally measure between 27 and 32 kilobases. The nucleocapsid protein [N] folds into a helical capsid that encloses the genome and is surrounded by an envelope. The viral envelope is composed of at least three structural proteins: the membrane protein (M), the envelope protein (E), and the spike protein (S) [3–6]. The M and E proteins are essential for virus production, while the S protein identifies which cells the virus prefers to infect [7, 8].

COVID-19 cases are diagnosed using a combination of patient symptoms and the real-time reverse transcription polymerase chain reaction examination of particular sequences of viral RNA (RT-PCR). RT-PCR is the most sensitive diagnostic approach [9]. While not commonly employed, atomic force microscopy has been utilized to determine the SARS-CoV virus's molecular structure and surface nanostructure [10, 11]. Strengthening one's immune system is crucial in the fight against infectious diseases. In this

Orhan Canbolat contributed equally to this work.

***Corresponding author: Prof. Dr. Orhan Canbolat**, Faculty of Medicine, Department of Medical Biochemistry, Gazi University, Ankara, Türkiye; and Life Sciences Application and Research Center, Gazi University Golbasi Campus, PK: 06830, Golbasi, Ankara, Türkiye, Phone: +905323869226, E-mail: ocanbolat@gazi.edu.tr. https://orcid.org/0000-0002-5916-2675
Fatih Canbolat, BilgiBiz Software, Hardware Ltd., Ankara, Türkiye. https://orcid.org/0009-0000-9203-0554
Mehmet Ali Ergün, Life Sciences Application and Research Center, Gazi University Golbasi Campus, Ankara, Türkiye; and Faculty of Medicine, Department of Medical Genetics, Gazi University, Ankara, Türkiye. https://orcid.org/0000-0001-9696-0433
Selin Yiğit, Faculty of Medicine, Department of Medical Microbiology, Gazi University, Ankara, Türkiye. https://orcid.org/0000-0001-7299-0822
Gülendam Bozdayı, Faculty of Medicine, Department of Medical Microbiology, Gazi University, Ankara, Türkiye; and Life Sciences Application and Research Center, Gazi University Golbasi Campus, Ankara, Türkiye. https://orcid.org/0000-0002-6036-6819

Open Access. © 2024 the author(s), published by De Gruyter. This work is licensed under the Creative Commons Attribution 4.0 International License.

respect, vaccination procedures play a crucial role in controlling the pandemic. Vaccines based on messenger RNA (mRNA) and DNA (DNA) as well as inactivated vaccines are commonly employed because they help the body develop immunity to the virus. Vaccines, on the other hand, have their efficacy reduced by the virus's ability to undergo genetic changes. Several treatments that are not designed to deal with COVID-19 are being tested out. Protease inhibitors like Lopinavir and RNA-dependent RNA polymerase (rdrp) inhibitors like Remdesivir and Favipiravir are used at the outset of these therapies [12]. The use of ultraviolet (UV) [13] or hypochlorous acid has been proposed to destroy viruses from the environment [14]. Despite this, there are several difficulties with using these methods. Because of its toxicity and the many different ways it may be put to use, using sodium hypochlorite to clean the environment on a large scale is not feasible. UV may weaken immune system, create cataracts, and even cause skin cancer, according to the World Health Organization [15]. Ultrasound has several non-medical applications, such as in manufacturing. Ultrasonic is a sort of wave that may pass through solid, liquid, or gaseous substances. It is in no manner comparable to radio waves or light waves [16]. Ultrasound sound waves may be a useful option for cleaning public spaces and air during the COVID-19 pandemic, compared to UV and hypochlorous acid.

In 1952, it was reported for the first time that ultrasound could clarify the molecular structure of DNA in aqueous solution [17]. Freifelder et al. provided support for the use of DNA as a test material to investigate the process of acoustic decay [18]. Ultrasonic waves degradation of DNA in aqueous solution, as seen by Elsner's team, involves the disruption of hydrogen bonds as well as single- and double-stranded breaks in the DNA helix. It has been hypothesized that a mechanical or thermal action is responsible for the destruction. Double-stranded oligonucleotides of different lengths in DNA solution were subjected to ultrasonic experiments by Basedow and his research group [19]. Cavitational processes in a liquid solution, as demonstrated experimentally, generate a mechanical-chemical reaction known as ultrasonic waves of DNA [20]. Serguei L. Grokhovsky and coworkers. He showed experimentally that the cleavage of double-stranded oligonucleotides of varying lengths and the fragmentation of the nucleic acid structure in a DNA solution may be caused by ultrasonic waves generated by a 300 W generator at a frequency of 22 KHz. Fragmentation of the DNA molecule occurs when the phosphodiester bond is broken. Electrophoresis was used to identify DNA fragments in this investigation [21]. All of this research looked at how *in vitro* ultrasonography affected the chemical bonding of nucleic acids in DNA structures. Ultrasound may have a disruptive impact on the membrane structure of SARS-CoV-2, as it has been shown that low frequency and low power ultrasound can disrupt the nucleic acid structure of RNA.

Tomasz Wierzbicki's theoretical work inspired our research topic [22]. Wierzbicki's discovery might have a revolutionary impact in controlling the COVID-19 pandemic if its models were tested in a controlled laboratory setting. For the present pandemic, Wierzbicki's hypothesis asked three key questions: (i) under what conditions does ultrasound induce large amplitude resonant vibrations of the crown and viral envelope? (ii) Does ultrasound stimulation interrupt the SARS-CoV-2virus life cycle without causing damage to normal cells? (iii) What mechanism allows for irreversible damage to spike proteins and viral shells? The geometry of the virus was used in computer simulations for this investigation. At 110 GHz, Wierzbicki shows significant alterations to the viral shell and spike protein structures. At 110 MHz, the viral envelope completely disintegrates in 0.35 ms, but at 50 MHz, it takes just 0.13 ms. This causes the viral envelope to develop pits and fissures. It is possible to interrupt the virus's life cycle by releasing RNA from the viral envelope. Extensive sections of the viral envelope were found to promote growth within the study's assumed safe range of 25–50 MHz. It has been reported that the ultrasound-induced fracture in the viral envelope began at the base of the spike and propagated upwards until the membrane broke. The viral membrane's integrity must be compromised, and the spike proteins must be dispersed throughout the membrane, for the virus to be rendered ineffective.

Flavio P. Veras' study showed that ultrasonic wave frequencies between 5 and 10 MHz were most effective for reducing SARS-CoV-2live particles [23]. Nevertheless, this study could not find evidence linking changes in nucleic acid structure to a decrease in viral activity. Importantly, our research corroborates the conclusions given by Flavio P. Veras and Wierzbicki. Our work uses RT-PCR and specialized cell culture techniques to show that low-frequency, low-power ultrasound application affects SARS-CoV-2 under *in vitro* settings.

In our study, the effect of ultrasound application at 8 W power and different frequencies on the virulence and proliferation rate of the SARS-COV-S virus was investigated.Due to the difficulties in developing a methodology to establish the disruptive effect of ultrasound on the membrane structure of the virus or the spike proteins in the lab, we evaluated the effect of ultrasound on the genetic structure of the virus using RT-PCR and cell culture in our investigation. We hypothesize that more improved dynamic laboratory techniques will allow us to examine the influence of ultrasound on the membrane and spike proteins of the virus under *in vitro* settings.

Materials and methods

The study's laboratory facilities were provided by the Gazi University Life Sciences Application and Research Center and the Virology Department at the Gazi University Training and Research Hospital. Researchers in the working group created the device's design and manufacturing process. Nasopharyngeal swab which was taken from two regions from nasal and pharyngeal were delivered to the Medical Virology Laboratory at the Gazi University Medical Faculty for PCR analysis of the COVID-19 virus. The specimens were collected in Viral Transport Medium (VTM, Bioeksen, Turkey) transfer tubes and transported to the laboratory where they were stored at 4 °C. Viral RNA was extracted using EZ1 Virus Mini Kit v2.0 on the automated EZ1 Advanced (Qiagen). A sample volume of 400 µL was used and the viral RNA was eluted in 60 µL. For the quality control of the extraction process, 2 µL of Genesig Easy RNA Internal Extraction Control was added to each sample. Following the extraction, real- time RT-PCR targeting the RdRp region of the SARS-CoV-2 genome was performed using Primer Design Genesig COVID-19 (Genesig). Rotor-Gene Q (Qiagen) was used in fluorescence channel Cycling Green for the detection of amplicons. Rotor-Gene Software was used to evaluate the amplification curves.

Manufacture and test model of ultrasound device

To create audible waves, a signal generator was developed. The digital generator can produce signals between 20 KHz and 200 MHz. The gadget was able to generate sound at 40 KHz, 25, 50, and 110 MHz. It was found that a potentiometer may be used to get the necessary frequency ranges for the sounds. Based on the amplifier we developed, the output sound signals may be amplified from 10 to 100 W, depending on user preference. The generated sound waves were broadcast using transducers that could operate at 40 KHz, 25, 50, and 110 MHz. The human ear is incapable of picking up these noises because of their high frequency. The Signal Generator was an Si5351 module. The I2C protocol is used for module control. The apparatus was set up on a sealed platform to direct the sound waves toward the intended recipient. The transducers send out sound waves that precisely hit the spot where the virus sample is. The target was exposed to 8 W of 40 KHz, 25, 50, and 110 MHz sound waves at distances of 10, 20, and 40 cm, respectively. Since in the preliminary study of our project, no effect of ultrasound 10, 20 and 40 cm applications on the results was observed, the results obtained from 10 cm are presented in the text. Tests were conducted by delivering 8 W of power for 1 min, with the target sample positioned at the designated location and the primary exit point of the sound source located 10 cm away. Several ultrasonic wave frequencies (40, 25, 50, and 110 MHz) were used in each experiment. Frequencies were applied uniformly to all samples. In each test, the device was activated and acoustic pulses were transmitted to the target for 1 min before being shut down.

Atomic force microscopy

After collecting samples from individuals diagnosed with COVID-19, the virus was distributed on slides and dried in a Class-2 laminar flow cabinet before being analyzed by ultrasonography and RT-PCR. The AFM (atomic force microscopy) testing was performed in the open air and contact mode. The analyses were performed beginning in a $100 \times 100\ mm^2$ region and zooming into a $10 \times 10\ mm^2$ region; the scanner's focal length is 150 mm. In the meanwhile, the applied force is 0.7 nN, and the image resolution is anywhere from 4,000 × 2,000 to 2,000 × 1,000 pixels; the data so collected is processed in software to produce a picture. We used AFM to examine the virus's membrane and protein architecture in this work (Figure 1).

Sample selection and real-time-PCR application

We received the samples in COPAN, UTM, and Italy transit containers with 2 mL of viral transport media. With the use of an EZ1 Advanced XL (Qiagen, Germany) instrument and an EZ1 Virus Mini Kit v2.0, nucleic acid was extracted from the samples in a completely automated fashion (Qiagen, Germany). The genesig® COVID-19 kit was used for the Real-Time qPCR analysis (PRIMER DESIGN, UK). The kit's sensitivity is optimized for the ORF1ab gene area, with a detection threshold of 0.33 copies/L. Four samples, all of which tested positive for COVID-19 DNA but with varying virus loads, were ultimately chosen for analysis.

Cell culture

The sample material in viral transport medium (VTM) frozen and kept at −80 C was placed in water bath at 36 C for 3–5 min and just after stored at −80 C deep freezer again. These dissolving and freezing process are repeated 3–4 times to succeed the release of the virus from its reservoir mammalian cells to be able to handle more free viruses. Then this virus containing viral transport medium was filled in a 15 mL Falcon tube and 5 mL DMEM or VTM was also added. Following placing it in water bath at 36 °C for a while, the Falcon tubes were centrifuged for 15 min at 3129 RCF. Using a sterile 0.20 mL syringe filter and sterile syringe, we transferred all of the supernatants from the falcon tubes into a DMEM-washed VERO E6 cell flask. The VERO E6 cell was inoculated with the SARS-CoV-2 RNA virus. Since the viruses can infect the VERO E6 cells in the absence of fetal bovine serum (FBS), the DMEM wash of VERO cells served to removing of existing FBS. After 37 min in an oven at 5 % CO_2, the flasks were taken out to control the cytopathic effect (CPE) process. Microscopical analysis of the flasks was performed every day for 7 days to monitor the development of CPE. Viral titration was determined by either CPU applying the formula established by Ramakrishnan MA et al. [24] and real-time PCR method.

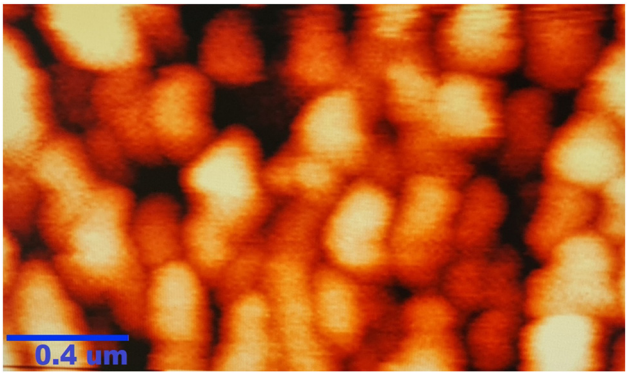


Figure 1: Image of SARS-COV-2 virus obtained by atomic force microscope.

Statistical analysis

The data of the research were analyzed with SPSS 23.0 (Social Sciences Statistical Package) program. Descriptive statistics were performed before data were evaluated. The conformity of continuous variables to normal distribution was evaluated using visual (histogram and probability plots) and analytical methods (Kolmogorov-Smirnov/Shapiro-Wilk tests). In the statistical analyzes in Tables 1 and 2, Median Value (min–max) values were used instead of Mean±Standard Deviation, and statistical analyzes were evaluated using Mann Mann-Whitney *U* and Wilcoxon tests. $p<0.05$ was considered statistically significant.

Ethics committee decision

Ethics committee decision of Gazi University Clinical Research Ethics Committee dated 31.05.2021 and numbered 579.

In addition, the notification made to the Ministry of Health before the study was approved by the Ministry.

Results

The threshold (Ct) for virus replication was determined before and after ultrasound treatment was applied to a collection of samples (Table 1). Ultrasound treatment resulted in an increase in the mean value of the RT-PCR viral cycle threshold (Ct) in the 40 KHz group. In contrast, viral Ct levels dropped in the 25 and 50 MHz groups following the ultrasonography. No statistically significant difference was seen between the pre-and post-ultrasound states of the 110 MHz group (Table 1).

Table 1: RT-PCR cycle threshold (Ct) before and after ultrasound application.

Groups	RT-PCR cycle threshold result before ultrasound application	RT-PCR cycle threshold result after ultrasound application	p-Value
	Median value (min–max)	Median value (min–max)	
40 Khz (n=9)	24.06 (22.74–25.29)	30.00 (29.00–30.00)	p=0.007[a]
25 Mhz (n=9)	26.33 (26.04–27.20)	18.00 (15.00–21.00)	p=0.007[b]
50 Mhz (n=9)	19.14 (18.71–19.56)	11.00 (11.00–15.00)	p=0.007[c]
110 Mhz (n=9)	16.43 (16.24–17.32)	16.00 (12.00–35.00)	p=0.857[d]

Wilcoxon test. [a]40 Khz p<0.01. [b]25 Mhz p<0.01. [c]50 Mhz p<0.01. [d]110 Mhz n.s.

Table 2: Replication number of SARS CoV 2 RNA virus in VERO E6 cell after ultrasound.

Groups	Median(min–max)	
40 KHz (n=4)	7.5 ± 5	10 (0–10)
25 MHz, (n=4)	300 ± 469	100 (0–1,000)
	p=0.178	
40 KHz (n=4)	7.5 ± 5	10 (0–10)
50 MHz (n=4)	775 ± 450	1,000 (100–1,000)
	p=0.015[a]	
40 KHz (n=4)	7.5 ± 5	10 (0–10)
110 MHz (n=4)	525 ± 550	550 (0–1,000)
	p=0.178	
25 MHz (n=4)	300 ± 469	100 (0–1,000)
50 MHz, (n=4)	775 ± 450	1,000 (100–1,000)
	p=0.155	
25 MHz (n=4)	300 ± 469	100 (0–1,000)
110 MHz (n=4)	525 ± 550	550 (0–1,000)
	p=0.647	
50 MHz, (n=4)	775 ± 450	1,000 (100–1,000)
110 MHz (n=4)	525 ± 550	550 (0–1,000)
	p=0.405	

Mann-Whitney *U* test. [a]p<0.05 40 KHz group compared with and 50 MHz group.

As shown in Table 2, after ultrasound application, the replication number of the SARS CoV 2 RNA virus in the VERO E6 cell was determined to be Median (min–max) 7.5 ± 5.0 10.0(0.0–10.0) in the 40 KHz group. In the statistical evaluation, a statistically significant difference was observed only between the averages of group 1 and group 3 ($p<0.05$). In cell culture, the growth rate of the virus was observed to be severely inhibited in the 40 KHz group. Nevertheless, in the 25, 50, and 110 MHz groups, replication rates were found to be higher than 40 KHz grops. In the 25, 50, and 110 MHz groups, these results demonstrated that ultrasound application did not inhibit the virus's proliferation. Only in the 40 KHz group was viral replication significantly reduced compared to the other groups.

The AFM analysis confirmed the viral envelope structure but failed to provide any evidence of spike proteins.

Discussion

In our study; ultrasound application in the 40 KHz group caused an increase in the mean value of the RT-PCR viral

cycle threshold (Ct). In contrast, viral Ct levels decreased in the 25 and 50 MHz groups. There was no statistically significant difference between the pre- and post-ultrasound conditions of the 110 MHz group (Table 1). It has been determined that 40 KHz ultrasound application inhibits the replication number group of the SARS-CoV-2 virus in the VERO E6 cell.

The genomic size of the SARS-CoV-2 virus ranges between 27 and 32 kilobase pairs [1, 2]. The envelope structure of the virus and the spike protein on the surface of the envelope have proven crucial factors in the onset of infection [3–8]. As a result of the membrane structure of the virus in the environment interfering with the function of the spike protein, the virus will have difficulty entering the host cell. This may be a crucial aspect in preventing infection. Instead, disruption to the nucleic acid structure and membrane structure of the virus may hinder the onset of infection. RNA viruses with a single strand are more responsive to ultrasound than DNA viruses. One of the fundamental theories is that ultrasound may be used to disrupt the nucleic acid structure of DNA. Several researchers have tested and published their findings on this notion [17–21]. Ultrasound with different frequencies and power is used for many different purposes in the field of medicine and production [25, 26].

It has been claimed that ultrasound may disrupt the phosphodiester bonds of DNA by causing the cavitation effect of the DNA molecule and reactive free radicals in the surroundings. In the *in vitro* liquid phase investigation, ultrasonic wave power levels as high as 300 W were employed [21]. There is limited information in the literature on application of ultrasound to disarm viruses that was found helpful in the present investigation, even though the keyword "ultrasound" was used in hundreds of papers [27]. Wierzbicki and colleagues tried to describe the effect of ultrasound on the spike protein structure of the virus at the atomic level [21, 27]. They used the molecular dynamics (MD) method to examine the interaction between atoms and the formation of molecules and proteins. The main difference of our study focused on how ultrasound affects the virulence and proliferation rate of the active virüs [27].

In our study, low-frequency and low-power ultrasound were favored over high-frequency and high-power ultrasound applications, which may be harmful to the environment or human health. In ultrasound applications, the intensity of the ultrasonic waves is just as crucial as their frequency. The pioneering work of Tomasz Wierzbicki et al., who modeled the action of ultrasound on the envelope and spike protein of the virus, provided light on our study endeavor. In contrast to the theoretical investigations of Tomasz Wierzbicki et al. In our study, the effect of a 40 kHZ and 8 w ultrasound sound effect on virulence and proliferation rate may be through the membrane structure of the virus, its effect on spike proteins, or an effect directly on the nucleic acid structure of the virus. RTPCs and cell culture results support this claim.

It can serve as a possible guide for the positive/negative diagnosis of SARS-CoV-2 in the clinic using Ct values. Typically, a low Ct suggests a large concentration of viral genetic material and an elevated risk of infectivity. It is stated that there is a clear relationship between low Ct values and the presence of clinical symptoms. In contrast, a high Ct implies a low concentration of viral genetic material, which is often correlated with a reduced chance of infection [28]. The most noteworthy findings of our study are the increase in Ct following ultrasound in the 40 KHz group and the reduction in the viral growth rate in cell culture. The detrimental effect of low-dose and low-power ultrasound on the virulence and proliferation rate of the virus might lead to the creation of a novel technique for limiting the COVID-19 pandemic. A cell culture study is the most crucial instrument for supporting the hypothesis of our research. Flavio's research demonstrates that SARS-CoV-2 activity decreases in the ultrasonic wave frequency range of 5–10 MHz [26]. Although the ultrasonic wave frequency range in the new study proposed by Feras differs from the 40 KHz frequency that prevents the virus from proliferating in our research, it is significant for demonstrating the effect of ultrasound on the rate of SARS-CoV proliferation. The results of Feras and our study indicate that additional research is required in this area. The primary distinction between our work and Flavion's is that the effect of ultrasound treatment on the viral load of SARS-CoV-2 is determined by Real-Time PCR. In the absence of clinical values, a single Ct value cannot be relied upon to determine the virus's transmissibility. According to the findings of our research, we believe it is more important to evaluate the viral activity and monitor the virus's replication rate in cell culture. Our notion is supported by Jian-statement Longu's that RT-PC has a clinical sensitivity of 79 % and a specificity of 100 %. In terms of demonstrating virus activity under laboratory conditions, cell culture studies are more significant experimentally, but their practical applications are limited. In clinical practice, the clinical compatibility of both RT-PCR and cell culture studies is essential.

The ultrasonic wave ranges used in our research are in the range of 5–100 [21, 23, 27], which were previously determined theoretically or practically in the literature. There is no accepted value about ultrasound frequency and power in the literature. In addition, ultrasound waves at the MHZ level were also used in our research in order to evaluate a wider area.

Another important difference of our study is that the wavelength used in the study was chosen in the low range. In

order to explain the effect of ultrasound on SARS COV-2 in more detail, we think that testing it at different low frequencies and powers will illuminate the subject better.

The preliminary results of our research indicate that the application of low-frequency and low-power ultrasound may be a practical and safe method for removing viruses from the environment. To further comprehend the impact of ultrasound on the nucleic acid or envelope structure of SARS-CoV-2, additional laboratory and experimental models are required. Our inquiry, which is a preliminary study, has produced ground-breaking information about this issue. This discovery may be crucial not only for the eradication of SARS-Cov 2 but also for the elimination of other RNA-containing viruses.

Conclusions

In vitro, ultrasound application at 40 KHz and 8w increased the Ct values of SARS-CoV-2 and decreased the viral growth rate in VERO E6 cells. The results of our preliminary study suggest that low-frequency, low-power ultrasound can be used as a new strategy to control the COVID-19 epidemic.

Acknowledgments: We appreciate Prof. Mithat Bozday's assistance with the cell culture procedure. In addition, we also thank Prof. Dr. Secil Ozkan's contributions to statistical analysis. The Turkish Patent Institute has registered the hypothesis part of this project and the device design with the number 824738 under the title "utility model application".

Research ethics: Ethics committee decision of Gazi University Clinical Research Ethics Committee dated 31.05.2021 and numbered 579. In addition, the notification made to the Ministry of Health before the study was approved by the Ministry.

Informed consent: Not applicable.

Author contributions: All authors have accepted responsibility for the entire content of this manuscript and approved its submission.

Competing interests: Authors state no conflict of interest.

Research funding: This research was funded by project code TCD-2021-7 from of the Gazi University Scientific Research Projects Coordination Unit ([BAP], https://doi.org/10.13039/501100003356).

Data availability: Not applicable.

References

1. Zhou P, Yang XL, Wang XG, Hu B, Zhang L, Zhang W, et al. A pneumonia outbreak associated with a new coronavirus of probable bat origin. Nature 2020;579:270–3.
2. Chan JF, Kok KH, Zhu Z, Chu H, To KK, Yuan S, et al. Genomic characterization of the 2019 novel human-path1ogenic coronavirus isolated from a patient with atypical pneumonia after visiting Wuhan. Emerg Microb Infect 2020;9:221–36.
3. Li F. Structure, function, and evolution of coronavirus spike proteins. Annu Rev Virol 2016;3:237–61.
4. Lan J, Ge J, Yu J, Shan S, Zhou H, Fan S, et al. Structure of the SARS-CoV-2 spike receptor-binding domain bound to the ACE2 receptor. Nature 2020;581:215–20.
5. Hofmann H, Pohlmann S. Cellular entry of the SARS coronavirus. Trends Microbiol 2004;12:466–72.
6. Vennema H, Godeke GJ, Rossen JW, Voorhout WF, Horzinek MC,, Opstelten, DJ, et al. Nucleocapsidindependent assembly of coronavirus-like particles by co-expression of viral envelope protein genes. EMBO J 1996;15:2020–8.,
7. Wrapp D, Wang N, Corbett KS, Goldsmith JA, Hsieh CL, Abiona O, et al. Cryo-EM structure of the -nCoV spike in the prefusion conformation. Science 2020;367:1260–3.
8. Huang Y, Yang C, Xu X-f, Xu W, Liu S-w. Structural and functional properties of SARS-CoV-2spike protein: potential antivirus drug development for COVID-19. Acta Pharmacol Sin 2022;41:1141–9.
9. Shen M, Zhou Y, Ye J, Abdullah AL-maskri A Ahmed, Kang Y, Zeng S, et al. Recent advances and perspectives of nucleic acid detection for coronavirus. J Pharm Anal 2020;10:97–1.
10. Lal R, John SA. Biological applications of atomic force microscopy. Am J Physiol 1992;266:C1–21.
11. Shiming Lin S, Chih-Kung Lee CK, Lee SY, Kao CL, Lin CW, Wang AB, et al. Surface ultrastructure of SARS coronavirus revealed by atomic force microscope. Cell Microbiol 2005;7:1763–70.
12. Umakanthan S, Kumar Chattu V, Ranade AV, Das D, Basavarajegowda A, Bukelo M. A rapid review of recent advances in diagnosis, treatment, and vaccination for COVID-19. AIMS Public Health 2021;8:137–53.
13. Loveday EK, Hain KS, Kochetkova I, Hedges JF, Robison A, Snyder DT, et al. Effect of inactivation methods on SARS-CoV-2virion protein and structure. Viruses 2021;13:562.
14. https://covid19.saglik.gov.tr/Eklenti/40447/0/covid19rehberi temasli takibi evde hasta izlemi ve filyasyon.
15. https://www.who.int/health-topics/ultraviolet-radiation#tab.
16. Zagzebski JA. Essentials of ultrasound physics, 1st ed. London: Mosly; 1996.
17. Laland SG, Overend WG, Stacey M. Deoxypentose nucleic acids. Part III. Some effects of ultrasonic waves on deoxypentose nucleic acids. J Chem Soc 1952;303–310. https://doi.org/10.1039/jr9520000303.
18. Freifelder D, Davıson PF. DNA studies on the sonic degradation of deoxyribonucleic acid. Biophys J 1952;2(3):235–247.
19. Elsner HI, Lindblad EB. Ultrasonic degradation of DNA. DNA 1989;8(10): 697–701.
20. Basedow AM, Ebert KH. Ultrasonic degradation of polymers in solution. In: Abe A, Albertsson A-C, Genzer J, editors. Advances in polymers science. Berlin/Heidelberg: Springer; 1997, 22:83–148 pp.
21. Grokhovsky SL, et al. Sequence-specific ultrasonic cleavage of DNA. Biophys J 2011;100:117–25.
22. Wierzbicki T, Li W, Liu Y, Zhu J. Effect of receptors on the resonant and transient harmonic vibrations of Coronavirus. J Mech Phys Solid 2021; 150:104369.
23. Veras FP, Martins R, Arruda E, Cunha FQ, Bruno OM. Ultrasound treatment inhibits SARS-CoV-2in vitro infectivity. BioRvix 2022;1–12. https://doi.org/10.1101/2022.11.21.517338.
24. Ramakrishnan MA. Determination of 50% endpoint titer using a simple formula. World J Virol 2016;5:85–6.

25. Ganidağlı E, Güze lR. Therapeutic ultrasound and effectiveness in knee osteoarthritis archives medical. Rev J 2013;22:170–83.
26. Moyano DB, Paraiso DA, Lezcano RAG. Possible effects on health of ultrasound exposure, risk factors in the work environment and occupational safety. Rev Health Care 2022;10:423.
27. Wierzbicki T, Bai Y. Finite element modeling of a-helices and tropocollagen molecules referring to spike of SARS-CoV-2. Biophys J 2022;121:2353–70.
28. Singh CV, Agarwal J, Garg J, Saquib M, Das A, Sen M. Role of cycle threshold of RT-PCR in the prediction of COVID-19. J Microbiol Infect Dis 2021;11:132–9.